Microelectronics Reliability 119 (2021) 114065

Contents lists available at ScienceDirect

Microelectronics Reliability

journal homepage: www.elsevier.com/locate/microrel

A comparative study of thermal fatigue life of Eutectic Sn-Bi, Hybrid Sn-Bi/SAC and SAC solder alloy BGAs

Chongyang Cai, Jiefeng Xu, Huayan Wang, S.B. Park *

Department of Mechanical Engineering, State University of New York at Binghamton, Binghamton, NY 13902, United States

ARTICLE INFO

Keywords:
Sn—Bi solder
Thermal cycling
Creep
Fatigue life

ABSTRACT

Low melting temperature solders are becoming a hot topic in Pb-free solder studies. Among these solders, Sn—Bi has attracted more attention because it can not only reduce the energy for reflow, but more importantly, increase the reliability of joints by minimizing warpage. In this study, the board-level reliability of the assembly of BGA components was investigated. Three types of assemblies are compared: mixed (hybrid) Sn-Bi/SAC305 assembly, which is made by soldering BGAs with SAC305 solder balls using eutectic Sn—Bi solder pastes so that the low reflow temperature avoids the SAC305 solder joints from being molten; homogeneous eutectic Sn—Bi assembly, which is made with solder balls and pastes that are both eutectic Sn-Bi; and homogenous SAC305 assembly as a control group. An accelerated thermal cycling test shows that homogeneous eutectic Sn—Bi assembly exhibits the best cycling reliability while the mixed assembly has the shortest fatigue life. The failure mechanism of the mixed assembly is also different from the other two types. Based on the experimental fatigue life results, the parameters of constitutive equation of eutectic Sn—Bi are calculated to evaluate the fatigue life of the solder joints. The study shows the better thermal cycling reliability of eutectic Sn—Bi assembly and help predict the fatigue life of different assemblies.

1. Introduction

Ball grid array (BGA) packages are widely used in surface mount manufacturing because they offer dense packaging and maintain good reliability with large amount of input/output counts [1]. Lead-free solder paste is widely used in BGA packages as an alternate for tin-lead solder to meet the environmentally friendly requirement. Among these lead-free solder pastes, Sn–Ag–Cu (SAC) solder has been the predominant choice because of its good reliability and solderability [2]. With the development of the packaging industry, low melting temperature solder is attracting more attention. A lower melting point requires a lower reflow profile temperature, which will save much more energy than SAC solders during the assembly. Sn—Bi is a very promising option for low melting temperature solder because of its unique advantages. First, the eutectic 58Bi—42Sn solder has a melting point as low as 138 °C, which is a big drop down from the melting point of 217 °C for SAC305. The much lower temperature will benefit heat-sensitive devices and protect organic materials inside the package [3]. Another advantage of Sn—Bi solder is its thermal expansion coefficient (CTE). Usually during the surface mounting process, the assembled packages will have warpages because of the thermal stress caused by the mismatched thermal expansion coefficient of solder joints and other materials [4]. The CTE of Sn—Bi is around 15 ppm/°C, which is very close to the substrates of components [5]. Such similarity will decrease the warpage of the package after the reflow process and make the manufactured samples more reliable.

In previous studies, researchers have investigated the Sn—Bi paste to compare it with other solders. From a thermal cycling perspective, applying Sn—Bi paste to assemble QFN packages has proved that samples using Sn—Bi paste have a better cycling resistance than those that use the SAC paste [6]. Other studies show the bonding of Sn—Bi joints exhibited similar improvements [7,8]. However, aside from thermal cycling experiments, some mechanical drop experiments show the opposite results: Sn—Bi solder joints generally fail earlier than other types of joints [9]. It is analyzed that Bismuth element in the paste will bring brittleness to the joints [10], furthermore, it may cause segregation at the interface between the copper pad and solder [11,12]. Those defects may be improved by adding third element dopants like Ag or Zn but the effect of Bismuth still cannot be neglected when considering the mechanical fatigue resistance [13,14]. When it comes to the studies of

* Corresponding author.
E-mail address: sbpark@binghamton.edu (S.B. Park).

https://doi.org/10.1016/j.microrel.2021.114065
Received 7 October 2020; Received in revised form 1 January 2021; Accepted 8 February 2021
Available online 26 February 2021
0026-2714/

Sn—Bi paste for BGA packages, most researchers employ SAC components and assemble them on PCB boards by applying with Sn—Bi paste. Those types of assembled joints are considered as mixed joints because the reflow temperature can only make Sn—Bi solder paste melt while the SAC305 solder balls on components will not melt and collapse. Those structures can help maintain a high standoff height of the joint [15].

In this study, to elucidate the reliability of the Sn—Bi solder, we assembled three types of packages: a mixed Sn-Bi/SAC assembly, a homogeneous eutectic Sn—Bi assembly, and a homogeneous SAC305 assembly. The mixed assembly was built with off-the-shelf components and solders, we substituted Sn—Bi for the SAC305 and manufactured a pure Sn—Bi package, and as a control group, we built packages with homogenous SAC305.

2. Experimental setup

Three types of components with different sizes and pitches are selected. The specs of these test vehicle components are listed in Table 1.

It is quite straightforward to mount available SAC components on boards using SAC paste or Sn—Bi paste so that homogenous SAC assembly and mixed assembly can be made. To manufacture the homogeneous Sn—Bi packages, stencil printing method is used to assemble the Sn—Bi components. Two methods are used to attach Sn—Bi solder balls on bare components. As shown in Fig. 1(a), the first method was used with CABGA160 and CABGA36, which have larger ball diameters and pitches than CVGBA432. The paste is printed on bare components first and then balls were attached to the paste through a stencil opening. After being heated at 175 °C for 5 min, the paste will combine with the solder balls and form homogenous Sn—Bi solder spheres. Components such as CVBGA432, have relatively much smaller ball sizes and pitches, and the first method takes much more time and may cause bridges. Thus, applying paste multiple times would be more convenient. Based on the volume calculation, the paste should be printed three times to make balls with comparable volume to SAC305 components for CVBGA432, as shown in Fig. 1(b).

After the Sn—Bi components are assembled, a bump inspection is performed to ensure that the assembled Sn—Bi components have comparable ball sizes as the available SAC components. As shown in Fig. 2 (a), using the first method, despite some deviations, the bump heights of Sn—Bi components are similar to SAC solder balls. As seen in Fig. 2(b) the second method increases the bump height by increasing the number of prints. For CVBGA432, with three times of printing, the bump heights of the Sn—Bi components are close to those of the SAC.

Fig. 3 shows the reflow profile of three types of assemblies, although there are only two curves as one curve represents two assemblies. For the homogeneous Sn—Bi assembly, the peak temperature is about 150 °C. The mixed assembly uses the same reflow profile as the homogenous Sn—Bi so that the Sn—Bi paste will melt while the SAC305 balls will not. The SAC305 melts at 217 °C. According to the time 0 x-ray picture after reflow shown in Fig. 4, there are no obvious huge voids inside the solder joints; therefore, the three types of assemblies can be considered as qualified.

All components and boards have internal daisy chains to make the assembly connected, as shown in Fig. 6. The time zero image of different solder balls at interface is shown in Fig. 5. For each type of component listed in Table 1, there are ten channels designed to inspect the resistance. Each channel has three components connected to one connector. Based on the resistance change information obtained from the connector, an in-situ inspection of component failures become feasible. All the homogeneous and mixed assemblies are put inside the same chamber to ensure they are under the same cycling condition. The cycling temperature range is from −40 °C to 125 °C, the ramp rate is set

Table 1
Specs of assembled components on boards.

Specs	CVBGA432	CABGA160	CABGA36
Dimension	13 × 13 mm	12 × 12 mm	6 × 6 mm
Thickness	0.65 mm	1 mm	1 mm
I/O Count	432	160	36
Diameter	0.25 mm	0.45 mm	0.45 mm
Pitch	0.4 mm	0.8 mm	0.8 mm

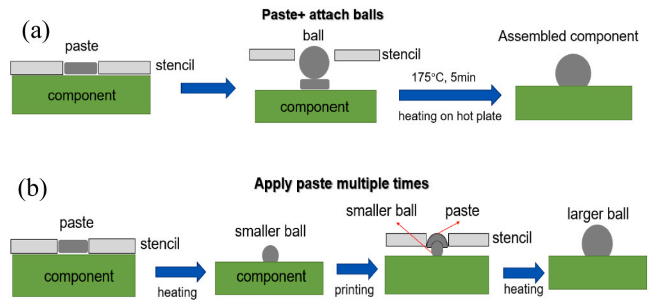

Fig. 1. Two methods of assembling solder spheres on bare components.

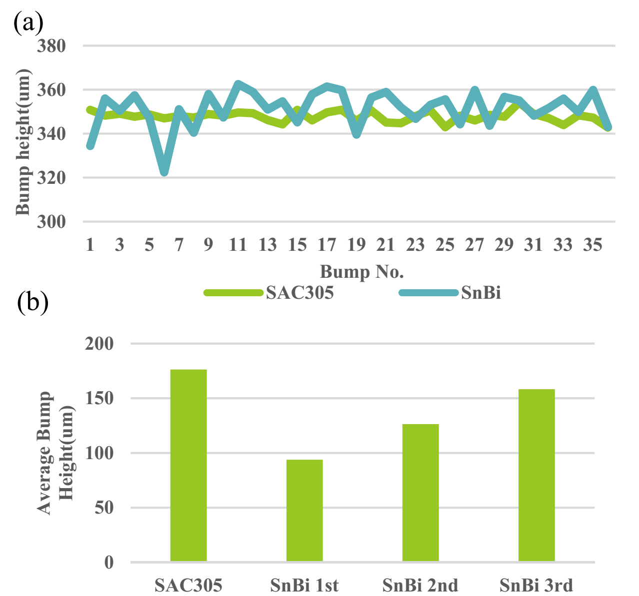

Fig. 2. Comparison of Sn—Bi components and SAC components, (a) bump height difference of two components using first method, (b)increase of bump height of Sn—Bi components by the second method.

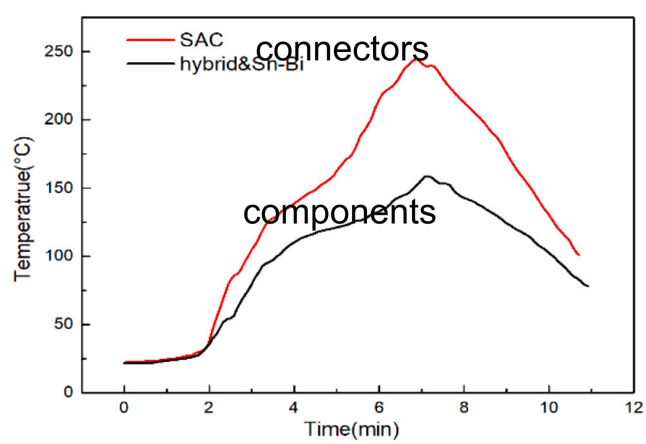

Fig. 3. Reflow profile of three types of assemblies.

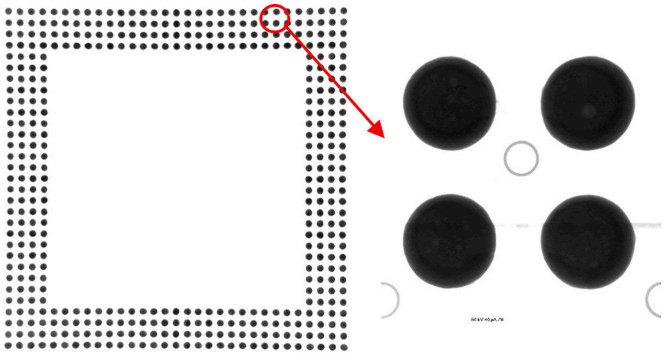

Fig. 4. X-ray inspection after the reflow.

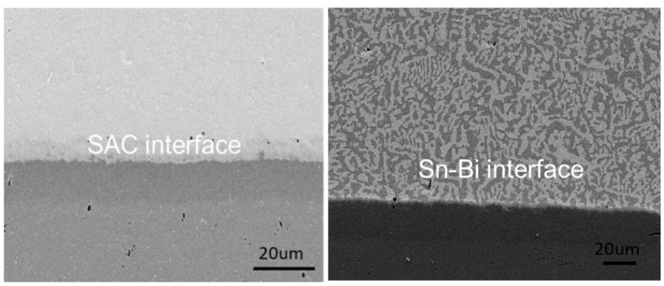

Fig. 5. Time zero image of interface at substrate side.

to 5 °C/min, and the dwell time is 20 min. The three boards inside the chamber are shown in Fig. 7.

3. Results and discussion

3.1. Fatigue test results

If the components have not failed, the resistance of the channel will follow the change of temperature. The peak resistance of each cycle will not change significantly. However, when cracks initiate and propagate inside the solder joints, the resistance will increase obviously. By monitoring the resistance, we can see when failure happens, as shown in Fig. 8. In this study, a 50% of peak increase is considered as failure.

During cycling, samples of joints are cross sectioned and observed under SEM microscope to observe the evolution of cracks. Fig. 9 shows the inside structure of different types of assembly joints at time 0 after the reflow, 1000 cycles,1250 cycles and 1500 cycles. From Fig. 9(a) we can see that after the reflow, SAC solder spheres in the mixed assembly will keep their shape as explained before. The failure mechanisms also vary between different assemblies. For the mixed assembly, the failure occurs mainly at the interface between the SAC sphere and Sn—Bi paste. The cracks will propagate along the interface and finally cause the failure of joints, and as a result the cracks will form near the PCB. In homogeneous assemblies, the situation is quite different. Homogeneous Sn—Bi and SAC solder will have cracks near the substrate side. Cycling fatigue resistance of these assemblies is also different. At 1000 cycles the mixed assembly already exhibits obvious cracks yet the homogeneous Sn—Bi and SAC assemblies did not show cracks until 1250 cycles. This phenomenon indicates that mixed assembly may have the shortest fatigue life and further quantitative study needs to be performed to confirm this observation.

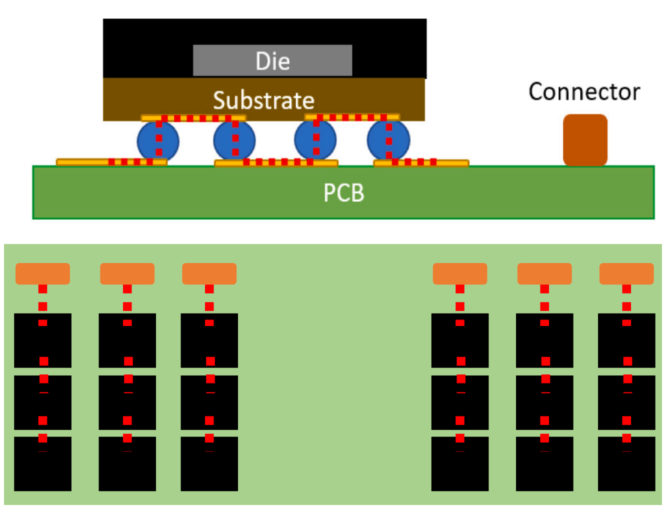

Fig. 6. Daisy chained structure of components and components on PCB boards.

Fig. 7. Assembled boards inside the cycling chamber.

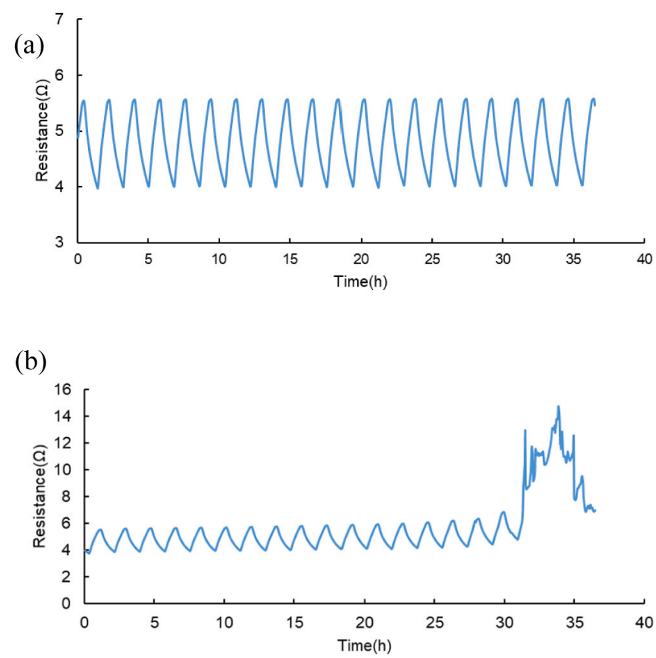

Fig. 8. Resistance change during the cycling, (a) component has no failure, (b) failure happens at solder joints.

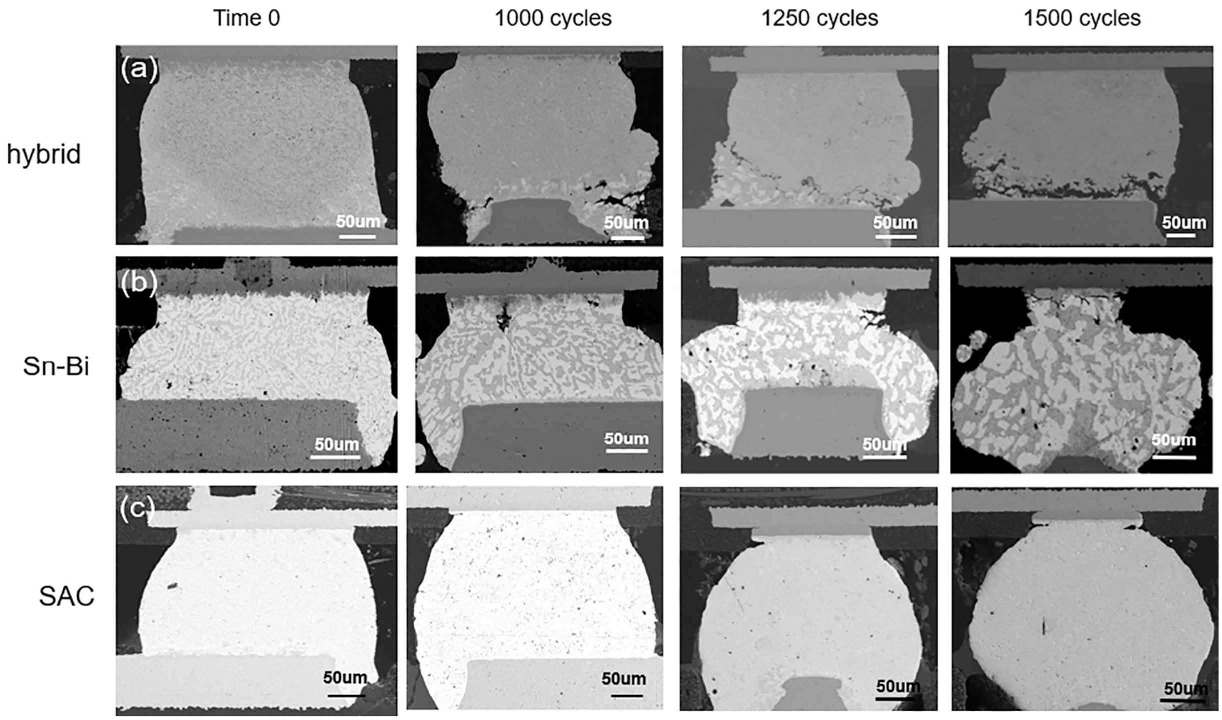

Fig. 9. SEM images of solder joints at different cycles, (a) mixed Sn-Bi/SAC joints, (b) Sn—Bi joints, (c) SAC joints.

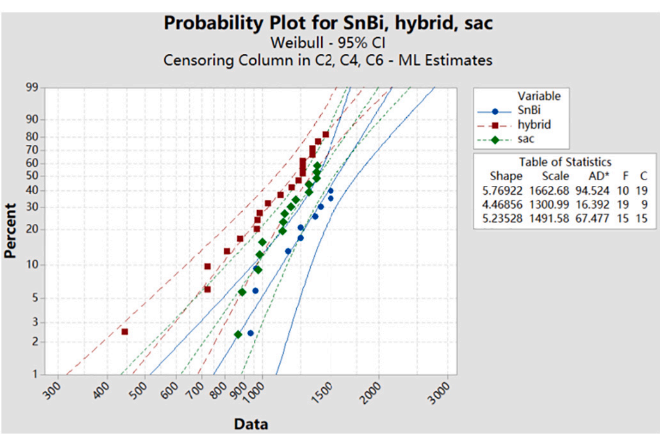

Fig. 10. Weibull plot of cycling results.

Fig. 10 shows the statistic result of all the assemblies after the 1500 thermal cycles. Among these components, CVBGA432 shows the most failures because it has the smallest ball diameter and pitch, a small number of CABGA160 failed and all CABGA36 components remained working through the experiment. Based on the study of CVBGA432, shown in Fig. 10, the homogeneous Sn—Bi assemblies are the most reliable packages, with a characteristic time to failure (TTF, 63.2%) is 1662 cycles; the homogenous SAC came in second, with TTF of 1491 cycles; and the hybrid joints show the shortest fatigue life, with a TTF of 1300 cycles. This can lead to the conclusion that the homogeneous Sn—Bi assembly usually has better thermal cycling resistance than the SAC, and the hybrid assembly will fail earlier than the two homogeneous ones, which is consistent with our previous SEM inspection.

3.2. Constitutive behavior of eutectic Sn—Bi solder

Based on the experimental results about the fatigue life of Sn—Bi solder, the prediction of fatigue life of different Sn—Bi assemblies become possible. However, it is necessary to obtain the constitutive equation of Sn—Bi solder so that the nonlinear behavior properties can be understood. The Anand model [16] is commonly used to describe the constitutive behavior of solder materials.

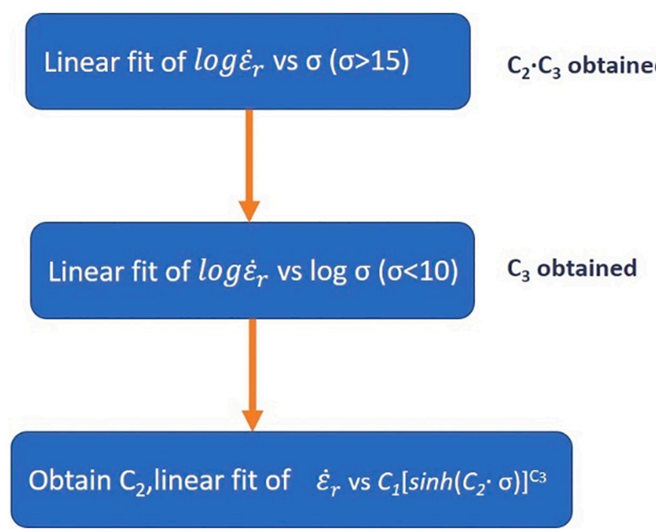

Fig. 11. Flow chart of obtaining constants by curve fitting.

$$\frac{d\varepsilon_p}{dt} = A[sinh(\xi\sigma/s)]^{1/m} exp\left(\frac{-Q}{kT}\right)$$

$$\frac{ds}{dt} = \left\{ h(|B|)^a \frac{B}{|B|} \right\} \frac{d\varepsilon_p}{dt}$$

$$B = 1 - \frac{s}{s^*} \quad s^* = \hat{s}\left[\frac{d\varepsilon_p/dt}{A} exp\left(\frac{Q}{kT}\right)\right]^n \quad (1)$$

Where $d\varepsilon_p/dt$ is the plastic strain rate, A is the pre-exponential factor, σ is

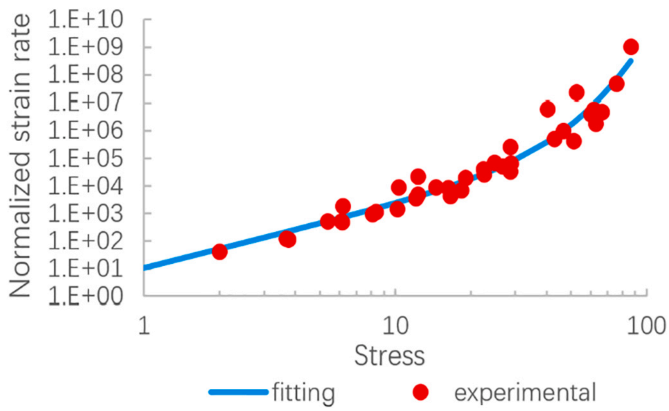

Fig. 12. Experimental results compared to fitted curve.

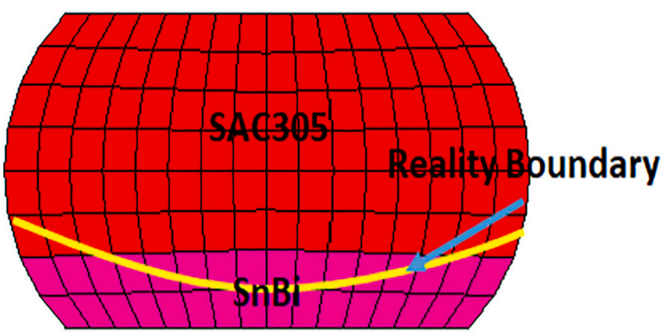

Fig. 13. FEA model of solder joints in mixed assembly.

the stress, ξ is the multiplier of stress, m is the strain rate sensitivity, k is the gas constant and Q is the activation energy of the solder, T is the absolute temperature, s is the internal variable and s^* is the saturation value [17].

In certain cases, this kind of equation can be simplified with a steady-state approximation. For low melting temperature solders, steady-state creep dominated the deformation kinetics, and the work hardening effects can be ignored [18]. As a result, the constitutive behavior of eutectic Sn—Bi solder joints can be described by the following Garofalo model [19]:

$$\frac{d\varepsilon_p}{dt} = A(sinh\beta\sigma)^n exp\left(-\frac{Q}{RT}\right) \tag{2}$$

The constants of the SAC305 solder in the Anand model and the Garofalo model are well understood from previous studies, yet there are no current data for the eutectic Sn—Bi solder, the only constant available is the activation energy, which is 0.63 eV [20]. As a result, the other three constants will be obtained based on the creep testing data of Sn—Bi solder.

Fig. 11 shows the flow chart for attaining the rest of the constants. When the stress is relatively large, the Garofalo equation can be rewritten as

$$\begin{aligned} \dot{\varepsilon}_n &= C_1\left[\frac{e^{C_2\sigma} - e^{-C_2\sigma}}{2}\right]^{C_3} \\ \dot{\varepsilon}_n &= C_1\left[\frac{e^{C_2\sigma}}{2}\right]^{C_3} \\ log\dot{\varepsilon}_n &= logC_1 + C_3 log\frac{1}{2} + C_3C_2\sigma \end{aligned} \tag{3}$$

where $\dot{\varepsilon}_n$ is the strain rate normalized by $exp\left(-\frac{Q}{RT}\right)$.

As a result, the C_2*C_3 value can be obtained.

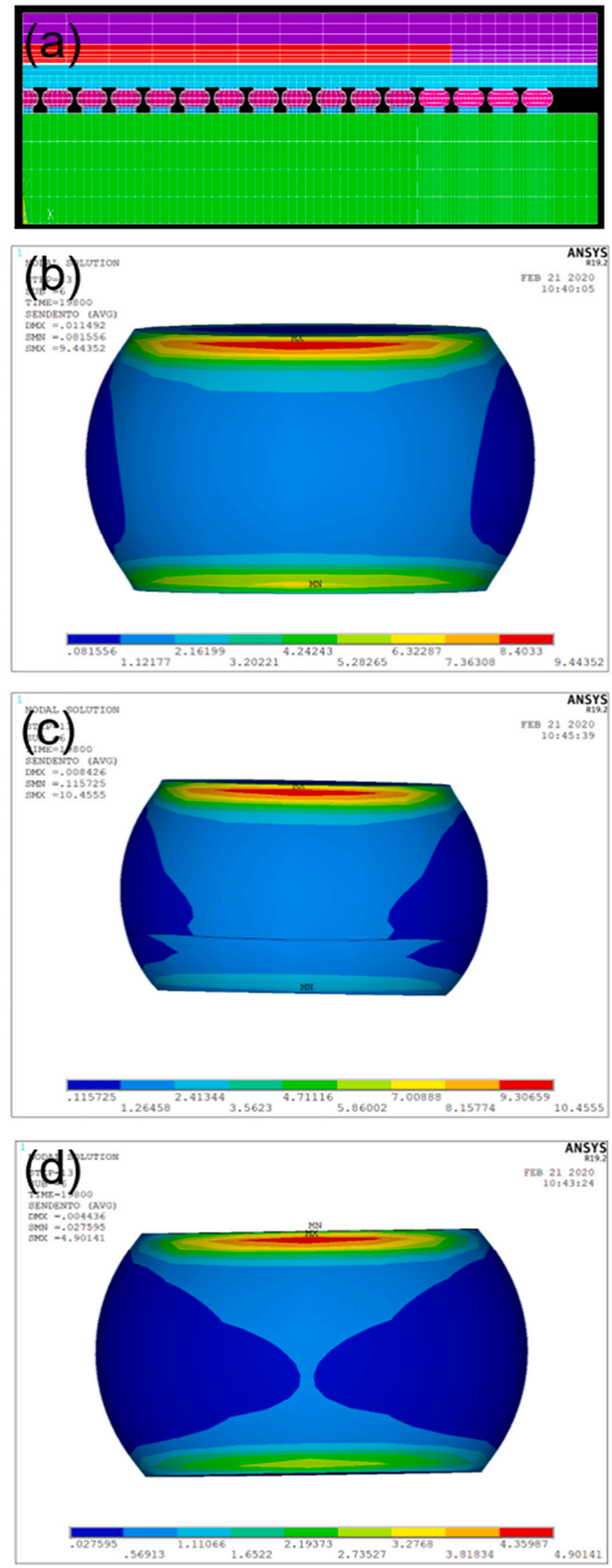

Fig. 14. (a) Sectional image of quarter symmetric model, energy distribution at critical solder: (b) SAC, (c) Mixed, (d) Sn—Bi.

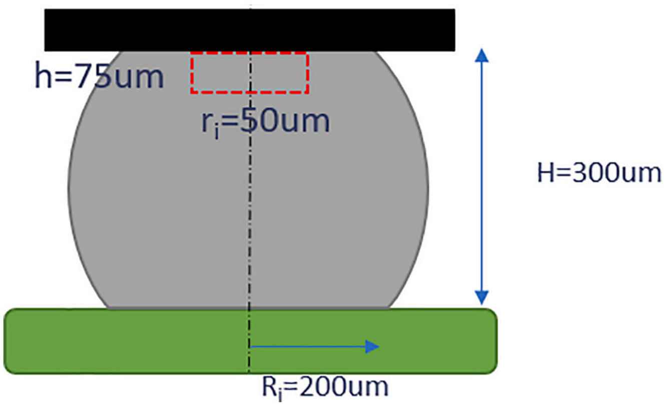

Fig. 15. Schematic of void inside the solder joint.

When stress is relatively small, the equation can be transformed to

$$Sinh(x) = x + \frac{x^3}{3!} + \frac{x^5}{5!} + \cdots$$

$$\dot{\varepsilon}_n = C_1[C_2\sigma]^{C_3}$$

$$log\dot{\varepsilon}_n = logC_1 + C_3 logC_2 + C_3 log\sigma \quad (4)$$

We can get C_3 value by curve fitting and thus C_2 value can also be calculated. Based on the historic experimental creep data of eutectic Sn—Bi solder in the literature, we can get the constants listed in Table 2. SAC305 constants are already available in the literature [20,21]. Based on the constants we can plot the fitting curve versus the experimental data as shown in Fig. 12.

3.3. Finite element analysis

According to the constitutive equation constants listed in Table 2, a finite element model can be built to analyze the nonelastic energy distribution inside the solder joints and predict the fatigue life of different assemblies. Based on the experimental observation in Fig. 9, the cracks will happen either at the top layer near the substrate side or the interface layer between the solder sphere and paste in the mixed case. Accordingly, the creep strain energy density accumulation will be calculated at the top layer and the interface for all three assemblies.

Darveaux put forward a model that is widely used to predict fatigue life based on the energy accumulation, which is [22]:

$$\alpha = N_0 + \frac{a}{da/dN}$$

$$N_0 = K_1(\triangle W_{ave})^{K_2}$$

$$\frac{da}{dN} = K_3(\triangle W_{ave})^{K_4} \quad (5)$$

Table 2
Constitutive constants in Garofalo model.

Solder	A(1/s)-C1	β/s(MPa-1)-C2	N-C3	Q/R(K)-C4
Sn42Bi58	6003	0.0627	2.29	6963
SAC305 [13]	2.91e-4	15.055	0.0179	3298.16

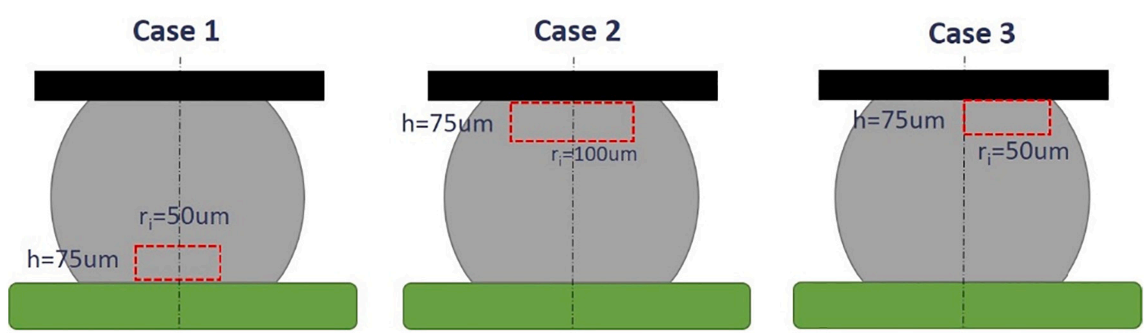

Fig. 16. Schematic of three different void cases.

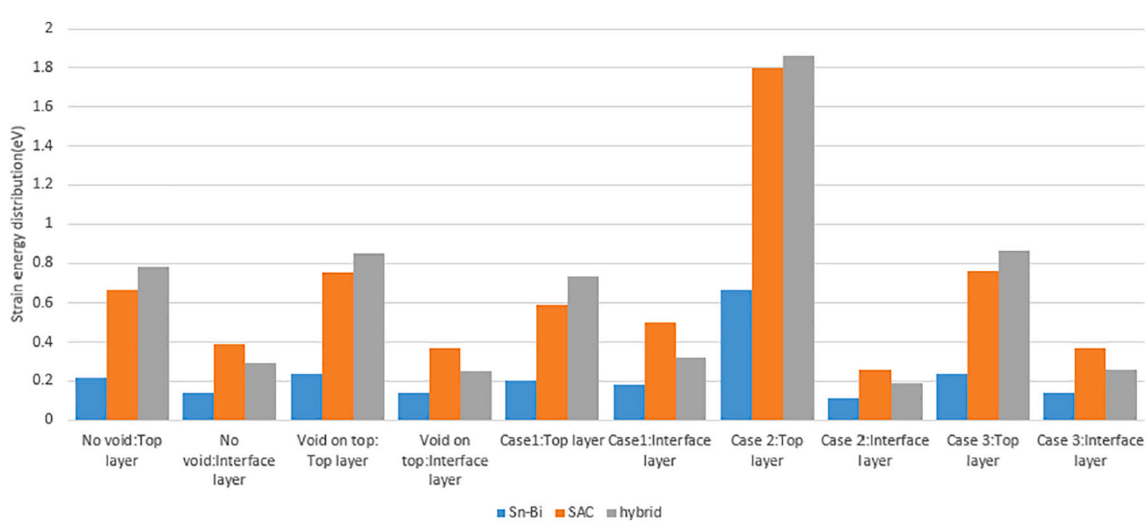

Fig. 17. Comparison of SED distribution for different void cases.

where α is the fatigue life, a is the opening window length, $da/dN$is the speed of crack propagation. N_0 is the number of cycles when cracks start to initiate, ΔW_{ave} is the accumulated energy density, K_1, K_2, K_3 and K_4 are fatigue related constants. Syed's model has made a further simplification [23]:

$$\alpha = c_1(\triangle W_{ave})^{-1} \tag{6}$$

The Syed model can be predict the fatigue life is because the crack initial cycles N_0 makes up less than 10% of the life time and can be neglected.

A quarter symmetric model of the package was built, for the mixed assembly's case, we change the interface between the SAC and the Sn—Bi from a typical, real-world curve to an idealized straight line, as shown in Fig. 13. The Strain Energy Distribution (SED) at the top layer and the interface location (at the interface between SAC305 and Sn—Bi but near the Sn—Bi side) are listed in Table 3. The energy distribution contour is plotted in Fig. 14. In actual cases, failure happens at the top of the paste in an Sn—Bi assembly at an energy level of 0.22, from which we calculate C_1. For homogeneous SAC assemblies, the failure happens at the top of the SAC305 at 0.67.

SnBi C_1: $1662 \times 0.22 = 365.64$
SAC305 C_1: $1491 \times 0.67 = 998.9$

For the mixed assembly, the top layer material is SAC305 and the interface layer material is Sn—Bi so the material constant for different layers is different.

Based on the constants from Sn—Bi, we can get the fatigue life prediction for the mixed assembly by applying Sn—Bi constant to the interface layer.

$$\alpha = 365.64 \times (0.293)^{-1} = 1248(\text{cycles})$$

The estimated life is close to the experimental results of 1300 cycles shown in Fig. 10.

The interface layer has shorter fatigue life, which is consistent with the fact that the crack will always start at the interface layer near the PCB instead at the top layer near the substrate side. The fatigue resistance does not only depend on the value of the SED, but also depends on the properties of the materials, which is related to the constant C_1.

3.4. Void evolution

Some voids inside the solder joints may also influence the vulnerability of the package [24,25]. To study the time 0 void effect on thermal cycling fatigue life, the area ratio and the height ratio of voids is assumed to be 25%. As shown in Fig. 15, a void with a diameter of 50 um, height of 75 um is planted within a solder with a diameter of 200 um, height of 300um. After adding the influence of the void, the SED distribution is listed in Table 4. With the updated energy accumulation, the fatigue life of mixed assembly can be calculated as:

$$\text{Top layer}: 998.9/0.85 = 1175.2$$

$$\text{Interface layer}: 365.64/0.25 = 1462.5$$

As listed in Table 4, for the mixed assembly, the top layer fatigue life is shorter than the fatigue life of the interfacial layer, and the crack will initiate at the top layer earlier than at the interface. According to Table 4, adding the void to solder joints may change the SED value, and it may increase the energy density on the top layer yet reduce the value on the interface layer. Such change may not only shorten the fatigue life of homogeneous assemblies but affect the failure mechanism in the mixed assembly.

Table 3
SED distribution at different assemblies.

Locations	Sn-Bi	SAC	Mixed
Top layer	0.22	0.67	0.78
Interface layer	0.14	0.4	0.293

Table 4
SED distribution at different assemblies after adding void influence.

Locations	Sn-Bi	SAC	Mixed
Top layer	0.244	0.75	0.85
Interface layer	0.14	0.37	0.25

Therefore, when there are voids inside the joints after the reflow, the SED distribution may change because of the voids. As a result, the failure mechanism of mixed assembly may change owing to the change of relationship between the top layer and the interface layer. Table 5 lists the value of both layers of each assembly, based on the calculation of Syed's constants,

If $998.9 \cdot (W_3)^{-1} < 365.6(W_3')^{-1}$, which means $W_3' < 0.37 * W_3$, failure will happen at substrate, otherwise it will at interface near the pad side.

A change of value in different solder assemblies may make a difference in fatigue life. If $998.9 \cdot (W_2)^{-1} < 365.6(W_3')^{-1}$, which means $W_3' < 0.37 * W_2$ SAC will fail earlier than the mixed assembly.

To further verify the influence of time 0 voids, three cases are studied as shown in Fig. 16. Case 1 moves the void shown in Fig. 15 from the top of the solder to the bottom near the PCB, Case 2 increases the void area, and Case 3 offsets the void.

The energy distribution comparison for the different cases is listed in Fig. 17. It can be seen that comparing to the previous void condition, when change the void location to the bottom layer near the PCB side, the top layer energy near the substrate side reduces and the energy at the interface layer increased. When increasing the void area ratio, the energy at the top layer will increase significantly. For the third case, changing the void offset will only have minor influence on the SED value.

4. Conclusion

In this study, three types of BGA assemblies-homogeneous Sn—Bi, homogeneous SAC and mixed Sn-Bi/SAC assemblies are compared under the same thermal cycling condition. A method based on stencil printing is put forward to manufacture components with Sn—Bi solder spheres. Based on the thermal cycling results, homogeneous Sn—Bi assembly shows the best thermal cycling resistance, homogeneous SAC the second, and the mixed assembly has the shortest fatigue life. The failure mechanism of the mixed assembly is also different. The cracks will emerge and propagate along the interface between the SAC sphere and the Sn—Bi paste near PCB. However, the homogenous SAC and Sn—Bi solder will have cracks at the top layer near the substrate side.

Constitutive equation and constants are determined for the eutectic Sn—Bi solder so that the fatigue life of BGA packages with similar assemblies can be predicted by finite element analysis. The investigation of void influence in the FEA model shows that the existence of voids after the reflow may change the fatigue life of packages and may affect the failure mechanism of the mixed assemblies.

CRediT authorship contribution statement

Chongyang Cai: Conceptualization, Methodology, Software, Formal analysis Investigation, Writing -original draft. **Jiefeng Xu:** Software,

Table 5
Parameters of SED distribution.

Locations	Sn-Bi	SAC	Mixed
Top layer	W_1	W_2	W_3
Interface layer	W_1'	W_2'	W_3'

Data curation. **Huayan Wang**: Validation, Formal analysis. **S.B. Park:** Resources, Supervision, Writing -review & editing, Funding acquisition.

Declaration of competing interest

The authors declare that they have no known competing financial interests or personal relationships that could have appeared to influence the work reported in this paper.

References

[1] Huayan Wang, et al., Product level design optimization for 2.5 D package pad cratering reliability during drop impact, in: 2019 IEEE 69th Electronic Components and Technology Conference (ECTC), IEEE, 2019.

[2] Dominik Herkommer, Jeff Punch, Michael Reid, A reliability model for SAC solder covering isothermal mechanical cycling and thermal cycling conditions, Microelectron. Reliab. 50 (1) (2010) 116–126.

[3] Hiren R. Kotadia, Philip D. Howes, Samjid H. Mannan, A review: on the development of low melting temperature Pb-free solders, Microelectron. Reliab. 54 (6–7) (2014) 1253–1273.

[4] Yuling Niu, et al., In-situ warpage characterization of BGA packages with solder balls attached during reflow with 3D digital image correlation (DIC), in: 2016 IEEE 66th Electronic Components and Technology Conference (ECTC), IEEE, 2016.

[5] Fay Hua, Zequn Mei, Judy Glazer, Eutectic Sn-Bi as an alternative to Pb-free solders. 1998 Proceedings. 48th Electronic Components and Technology Conference (Cat. No. 98CH36206), IEEE, 1998.

[6] Bart Vandevelde, et al., Improved QFN thermal cycling reliability using low melting temperature SnBi based solder paste LMPA-Q, in: 2019 20th International Conference on Thermal, Mechanical and Multi-Physics Simulation and Experiments in Microelectronics and Microsystems (EuroSimE), IEEE, 2019.

[7] Rui Zhang, et al., Tin-bismuth plating for component finishes, in: 2011 IEEE 61st Electronic Components and Technology Conference (ECTC), IEEE, 2011.

[8] Liu, Yan, et al. "Reliability of BGA assembled with lead-free low melting and medium melting mixed solder alloys." 2014 15th International Conference on Electronic Packaging Technology. IEEE, 2014.

[9] Jianhui Wang, et al., Mechanical properties and joint reliability improvement of Sn-Bi alloy, in: 2011 IEEE 13th Electronics Packaging Technology Conference, IEEE, 2011.

[10] Y. Wasserman, Integrated single-wafer RP solutions for 0.25-micron technologies, IEEE Trans-CPMT-A 17 (3) (1995) 346–351.

[11] Q.L. Yang, Jian Ku Shang, Interfacial segregation of Bi during current stressing of Sn-Bi/Cu solder interconnect, J. Electron. Mater. 34 (11) (2005) 1363–1367.

[12] Chih-Ming Chen, Long-Tai Chen, Ya-Shiu Lin, Electromigration-induced Bi segregation in eutectic SnBi solder joint, J. Electron. Mater. 36 (2) (2007) 168–172.

[13] Wenxing Dong, et al., Effects of trace amounts of rare earth additions on microstructure and properties of Sn-Bi-based solder alloy, J. Electron. Mater. 37 (7) (2008) 982–991.

[14] Q.S. Zhu, et al., Effect of Zn addition on microstructure of Sn-Bi joint, in: 2009 International Conference on Electronic Packaging Technology & High Density Packaging, IEEE, 2009.

[15] Robert Kinyanjui, et al., Solder joint reliability of Pb-free SnAgCu ball grid Array (BGA) components in SnPb assembly process, Proceedings of APEX 2008 (2008) S15–2.

[16] M. Anand, K.R. Rajagopal, A shear-thinning viscoelastic fluid model for describing the flow of blood, International Journal of Cardiovascular Medicine and Science 4 (2) (2004) 59–68.

[17] Munshi M. Basit, et al., The effects of aging on the Anand viscoplastic constitutive model for SAC305 solder, in: Fourteenth Intersociety Conference on Thermal and Thermomechanical Phenomena in Electronic Systems (ITherm), IEEE, 2014.

[18] Z.N. Cheng, et al., Viscoplastic Anand model for solder alloys and its application, Soldering & Surface Mount Technology 12 (2) (2000) 31–36, https://doi.org/10.1108/09540910010331428.

[19] Frank Garofalo, Fundamentals of Creep and Creep-Rupture in Metals, Macmillan, 1965.

[20] C.H. Raeder, D. Mitlin, R.W. Messler, Modelling the creep rates of eutectic bi–Sn solder using the data from its constitutive phases, J. Mater. Sci. 33 (18) (1998) 4503–4508.

[21] Zequn Mei, Helen A. Holder, Hubert A. Vander, Plas, Low-temperature solders, Hewlett Packard Journal 47 (1996) 91–98.

[22] R. Darveaux, Effect of simulation methodology on solder joint crack growth correlation, in: 2000 Proceedings. 50th Electronic Components and Technology Conference (Cat. No. 00CH37070), IEEE, 2000, May, pp. 1048–1058.

[23] Ahmer Syed, Updated life prediction models for solder joints with removal of modeling assumptions and effect of constitutive equations, in: EuroSime 2006-7th International Conference on Thermal, Mechanical and Multiphysics Simulation and Experiments in Micro-Electronics and Micro-Systems, IEEE, 2006.

[24] Xu, Jiefeng, et al. "Time 0 Void Evolution and Effect on Electromigration." 2019 IEEE 69th Electronic Components and Technology Conference (ECTC). IEEE, 2019.

[25] Leila Jannesari Ladani, Abhijit Dasgupta, Effect of Voids on Thermomechanical Durability of Pb-free BGA Solder Joints: Modeling and Simulation, 2007, pp. 273–277.